



Published in final edited form as:

Am J Psychiatry. 2009 September ; 166(9): 1011–1024. doi:10.1176/appi.ajp.2009.08121760.

A Molecular Signature of Depression in the Amygdala

Etienne Sibille, Ph.D., Yingjie Wang, M.S., Jennifer Joeyen-Waldorf, B.S., Chris Gaiteri, B.S., Alexandre Surget, Ph.D., Sunghae Oh, B.S., Catherine Belzung, Ph.D., George C. Tseng, Ph.D., and David A. Lewis, M.D.

From the Department of Psychiatry and Biostatistics and the Center for Neuroscience, University of Pittsburgh; and CNRS, INSERM, and Université François Rabelais, Tours, France.

Abstract

Objective—Major depressive disorder is a heterogeneous illness with a mostly un-characterized pathology. Recent gene array attempts to identify the molecular underpinnings of the illness in human postmortem subjects have not yielded a consensus. The authors hypothesized that controlling several sources of clinical and technical variability and supporting their analysis with array results from a parallel study in the unpredictable chronic mild stress (UCMS) rodent model of depression would facilitate identification of the molecular pathology of major depression.

Method—Large-scale gene expression was monitored in postmortem tissue from the anterior cingulate cortex and amygdala in paired male subjects with familial major depression and matched control subjects without major depression (N=14–16 pairs). Area dissections and analytical approaches were optimized. Results from the major depression group were compared with those from the UCMS study and confirmed by quantitative polymerase chain reaction and Western blot. Gene coexpression network analysis was performed on transcripts with conserved major depression-UCMS effects.

Results—Significant and bidirectional predictions of altered gene expression were identified in amygdala between major depression and the UCMS model of depression. These effects were detected at the group level and also identified a subgroup of depressed subjects with a more homogeneous molecular pathology. This phylogenetically conserved “molecular signature” of major depression was reversed by antidepressants in mice, identified two distinct oligodendrocyte and neuronal phenotypes, and participated in highly cohesive and interactive gene co-expression networks.

Conclusions—These studies demonstrate that the biological liability to major depression is reflected in a persistent molecular pathology that affects the amygdala, and support the hypothesis of maladaptive changes in this brain region as a putative primary pathology in major depression.

Although we know that dysregulated serotonergic and stress pathways are contributing factors in major depressive disorder, and despite the passage of more than 50 years since the discovery of clinically effective antidepressants, the biological mechanisms of major depression remain mostly uncharacterized (1). Recent attempts to identify the molecular pathology of the illness based on large-scale gene arrays have implicated several biological

Address correspondence and reprint requests to Dr. Sibille, Department of Psychiatry, University of Pittsburgh, 3811 O'Hara St., BST W1643, Pittsburgh, PA 15213; sibilleel@upmc.edu.

Presented in part at the 37th annual meeting of the Society for Neuroscience, San Diego, Nov. 3–7, 2007, and at the 63rd annual scientific meeting of the Society of Biological Psychiatry, Washington, D.C., May 1–3, 2008.

Dr. Belzung has served as a consultant to Takeda. Dr. Lewis has received research support from the Bristol-Myers Squibb Foundation, Curidium Ltd, Merck, and Pfizer and has served as a consultant to Astra-Zeneca, Bristol-Myers Squibb, Merck, Pfizer, Roche, Sepracor, and Wyeth. All other authors report no competing interests.

systems but have not yielded a consensus, possibly because of differences in cohorts, brain areas investigated, and analytical approaches (2–6) as well as a substantial clinical heterogeneity. In fact, major depressive disorder may correspond to a family of disorders, which may be identified based on more narrow clinical and biological definitions (7).

We sought to address these challenges in a gene expression profiling study of major depression designed 1) to reduce the clinical heterogeneity of the human cohort, 2) to focus on a relevant neural network, 3) to control for the variability in gene expression intrinsic to each brain region, 4) to maximize true discovery in gene array approaches, and 5) to use a parallel study in a more tractable animal model of depression and antidepressant reversal to support the analysis of the human results. The unpredictable chronic mild stress (UCMS) rodent model is informative for studying depression in animals, as it mimics in a naturalistic way the role of psychosocial environmental stressors in precipitating a depressive pathology and the time frame of antidepressant response (8,9). The random application of several environmental and social mild stressors for several weeks results in a syndrome that is reminiscent of symptoms of depression, including physiological changes, increased fearfulness/anxiety-like behavior, and altered agonistic behavior (9).

Our studies focused on the anterior cingulate cortex and the amygdala as critical components of a corticolimbic circuit of mood regulation (10) that is affected in major depression (11). Evidence supporting dysfunctions of these areas in major depression include decreased anterior cingulate cortex volume and altered activity (12–15), decreased glial density and reduced (16) or no change in neuronal size (17) in the anterior cingulate cortex, decreased glial density (18) and fewer oligodendrocytes (19) in the amygdala, and abnormal processing of emotional stimuli and sustained amygdala reactivity (20–22). Accordingly, we tested the hypothesis that the biological liability to major depression would be reflected in a persistent molecular pathology affecting the amygdala and/or the anterior cingulate cortex.

Method

Subjects

Brain samples were obtained during autopsies conducted at the Allegheny County Medical Examiner's Office (Pittsburgh) after consent was provided by next of kin. Consensus DSM-IV diagnoses were made by an independent committee of experienced clinical research scientists using information from clinical records, toxicology results, and a standardized psychological autopsy. We analyzed 16 pairs (14 in the amygdala), consisting of white male subjects with familial major depressive disorder and control subjects without major depression matched for age, sex, and race (Table 1). The increased disease severity was supported by a longer average duration of illness in the familial depression cohort compared to subjects with nonfamilial major depression from the same brain donation program (mean duration, 9 years [SD=7.0] compared with 3 years [SD=3.9], $p=0.01$). A symptom score was calculated based on the presence at time of death (1= unequivocal yes; 0.5=unsure or subthreshold; 0=unequivocal no) of nine symptoms of major depressive disorder: depressed mood, anhedonia, appetite disturbance, sleep disturbance, psychomotor change, anergia, self-recrimination, diminished ability to concentrate or make decisions, and suicidality. All procedures were approved by the University of Pittsburgh's Institutional Review Board and Committee for Oversight of Research Involving the Dead. Detailed information is available in the data supplement that accompanies the online edition of this article.

Brain Samples

Rostral amygdala samples enriched in lateral, basolateral, and basomedian nuclei were delineated as described elsewhere (19) and dissected from frozen coronal blocks ~2–3 cm

caudal to the temporal pole. Samples of anterior cingulate cortex containing all six cortical layers were harvested from coronal sections in the subgenual anterior cingulate. A pilot study revealed rostrocaudal variations in transcript levels in both areas (Figure 1A,B). Selected white matter samples from anterior cingulate cortex (N=7) and amygdala (N=4) were obtained for analysis of cellular origin of transcripts (23).

Microarray Samples

Total RNA was extracted from frozen samples stored in TRIzol (Invitrogen, Carlsbad, Calif.) and processed for microarray analysis according to the microarray manufacturer's protocol (Affymetrix, Santa Clara, Calif.). In brief, 2.5 µg of total RNA was reverse-transcribed and converted into double-stranded cDNA. A biotinylated cRNA was transcribed in vitro, using an RNA polymerase T7 promoter site introduced during the reverse-transcription step. Twenty micrograms of fragmented labeled cRNA sample were hybridized onto Human Genome U133Plus-2.0 arrays, assessing 54,675 probesets or gene transcript levels. To reduce the influence of technical variability, paired samples were processed together, but different pairs were randomly distributed at each experimental step. For samples, hybridization, and array quality control, probeset signals (i.e., transcript levels) were extracted with the Affymetrix GCOS software. For statistical analysis, log₂-transformed probeset signal intensities were extracted and normalized with the robust multiarray average (GC-RMA) algorithm (24). Probesets with GC-RMA data values below 12 displayed systematic coregulation patterns corresponding to the array normalization procedure and were considered background signal, leaving 25,859 probesets with detectable signal in the anterior cingulate cortex and/or the amygdala.

Control Group					
Case	Age (Years)	Postmortem Interval (Hours)	pH	Storage (Months)	RNA Integrity Number
685	57	14.0	6.6	98	8.0
789	23	20.0	7.0	80	7.4
795	69	12.0	6.6	102	8.2
615	62	7.2	6.4	108	7.8
551	62	16.4	6.6	118	8.3
634	53	16.0	7.0	105	8.1
713	58	37.5	7.0	94	8.4
736	55	15.5	6.9	88	8.3
1086	51	24.2	6.8	27	8.1
857	48	16.6	6.7	66	8.9
1122	56	15.4	6.7	49	7.9
852	54	8.0	6.8	36	9.1
1067	49	6.0	6.6	77	8.2
1031	54	23.1	6.8	35	8.2
604	39	19.3	7.1	108	8.6
1047	43	12.0	6.9	32	9.0
	51.6	16.5	6.7	73.0	8.3
	11.3	8.2	0.2	32.3	0.4
	52.0	16.5	6.8	76.3	8.2

Control Group					
Case	Age (Years)	Postmortem Interval (Hours)	pH	Storage (Months)	RNA Integrity Number
	10.7	7.7	0.2	31.5	0.6

Microarray Quality Control

Individual scans were visually inspected for the presence of manufacturing defaults and hybridization artifacts. Quality control parameters were as follows: noise (RawQ, anterior cingulate, 1.47 [SD=0.34]; amygdala, 1.47 [SD=0.34]), background (anterior cingulate, 44 [SD=8]; amygdala, 43 [SD=5]), scale factor (anterior cingulate, 2.62 [SD=1.32]; amygdala, 4.41 [SD=0.97]), 3'/5' actin ratio (anterior cingulate, 2.97 [SD=0.98]; amygdala, 2.98 [SD=0.93]), and 3'/5' glyceraldehyde 3-phosphate dehydrogenase ratio (anterior cingulate, 1.23 [SD=0.217]; amygdala, 1.45 [SD=0.28]). Consistent numbers of genes were detected across arrays (anterior cingulate, 46.8% [SD=2.2]; amygdala, 48.2% [SD=3.3]), and consistent detection of BioB/C hybridization spiked controls. To further identify outlier samples, we used the “outlier detection” feature of the DNA-Chip Analyzer software (<http://www.biostat.harvard.edu/complab/dchip>), and analyzed correlation coefficients between array signals across all samples. Based on these results, 16 pairs were retained for analysis in anterior cingulate cortex and 14 pairs in amygdala.

Rodent UCMS Model

We previously described a behavioral and microarray study in the UCMS model of depression in mice (9). Behavioral and array results from that study were used here to support the analysis of data in the homologous brain areas in human subjects. In brief, BALB/c mice were subjected to various stressors according to a pseudorandom schedule for 7 weeks. Drug (fluoxetine, 20 mg/ kg/day, or a corticotropin-releasing-factor 1 [Crflr] antagonist [SSR125543], 20 mg/kg/day) or vehicle treatments started on day 14 and continued until the end of UCMS, when microarray data (MOE430-2.0) were generated in cingulate cortex and amygdala (lateral/basolateral nuclei). Stressors included altered bedding (sawdust change, removal, or damp; substitution with water, rat, or cat feces); cage tilting or shaking; cage exchange (mice exposed to the empty cage of another male); induced defensive posture (repeated slight grips on the back); and altered light/ dark cycle. Body weight and coat state were assessed weekly, as markers of the progression of the UCMS-evoked syndrome. The coat score combined results from different body parts (0=well-groomed, 1=unkempt). This index has been pharmacologically validated (25). Emotion-related and agonistic behaviors were measured at the end of UCMS using the novelty suppressed feeding test and the resident/intruder test. The novelty suppressed feeding test consists of providing food-deprived mice with a food pellet in a novel, aversive environment (a brightly lit enclosure). The latency to start feeding correlates with fearfulness and decreases after acute treatment with anxiolytic drugs (26) or chronic antidepressant exposure (25), suggesting that mechanisms underlying changes in the latency to feed involve anxietylike and depression-like processes. For the resident/intruder test (27), control and UCMS-treated mice were single-housed in new cages 2 days before testing. The opponent, a 6-month-old BALB/ c intruder, was placed into the home cage of the test animal (resident). Latencies and number of attacks were recorded for 10 minutes. Detailed methods and results are described in (9) and summarized in Table 2.

White Matter/Gray Matter Analysis

Ratios of transcript levels between white matter and gray matter samples were generated as described and used as estimates of relative gene transcript enrichment in glia (white matter/gray matter >1.5), neurons (white matter/gray matter <-1.5), or both cellular populations (-1.5 < white matter/gray matter < 1.5) (23). (See the online data supplement for details.)

Array Data Statistical Analysis

Selection of significant genes—To maximize discovery, we opted for an analytical approach with initial low stringency, followed by a comparative analysis with UCMS array data. First we flagged any gene potentially affected in correlation with major depression, and then we focused on cross-species identification of similar changes for orthologous probesets. The assumption was that major-depression-related changes would manifest as weak effects but that the conservation of such changes across species would provide independent lines of validation and thus facilitate their identification from background variability or unrelated changes. We previously validated this approach in a study of gene expression correlates of aging between human and mouse brain (28).

Statistical criteria—Changes in gene expression can take different nonexclusive forms in large data sets and are difficult to assess with any single test. Thus, for our inclusive first step, genes were tested by parametric paired t test, nonparametric paired Wilcoxon signed-ranks test, and analysis of variance (ANOVA), as well as taking into consideration several clinical covariate parameters. In ANOVA, the observed variance was partitioned into components explained by different explanatory variables (covariates). We applied the following ANOVA model for each gene:

$$Y_{gi} = \alpha_g + \beta_g * S_i + \tau_g * R_i + \gamma_g * A_i + \delta_g * AD_i + \varepsilon_{gi},$$

where $1 \leq g \leq G = 26,199$ genes, $1 \leq i \leq I$ pairs, and with clinical covariate values of 1 if the condition is true and 0 otherwise (S_i , suicide; R_i , recurrence; A_i , comorbid alcohol dependence; AD_i , antidepressant). Since some of the covariates may not be statistically significant for each gene g , we applied a stepwise model selection by the Akaike information criterion (29) to find the final “best fit” model, and a corresponding adjusted p value was calculated for each gene. Genes were selected if any of the three statistical criteria were less than 0.05 and if group differences in transcript levels (paired and unpaired) were greater than 20% using mean or median averaged values, corresponding to a difference at the low limit of quantitative polymerase chain reaction (qPCR) confirmation. Genes were selected according to similar criteria in the UCMS data set (ANOVA, $p < 0.05$; changes >20%) (9). The significance of the cross-species concordance was assessed by bootstrap resampling (using the same analytical procedures), where sample groups were repeatedly shuffled in equal proportion (control and experimental), thus removing the major depression or UCMS component from the analysis. The procedure was repeated 1,000 times to generate a null distribution so that p values of the observed directional correlations could be assessed.

Directional correlations, $r(D_1, D_2)$, were calculated in a pair of cross-species or cross-brain region data sets D1 and D2. Ortholog probesets were identified using the Netaffx webtool (Affymetrix, Inc.) to link the human and mouse data sets. In contrast to traditional Pearson correlation, the directional correlation measures the fitness of significant genes in D1 to predict D2, and conversely of D2 to predict D1. For instance, the statistically significant genes in D1 were first selected and the Pearson correlation of the log-ratios of D1 and D2 in this restricted D1-significant gene set was calculated. Thus, directional correlations are not symmetric ($r[D1, D2] \neq r[D2, D1]$).

Group variability in gene expression was assessed by two-group t test using individual gene transcript variances as continuous variables.

Real-Time qPCR

qPCR was performed as previously described (28). Results were calculated as the geometric mean of relative intensities compared to three internal controls (actin, glyceraldehyde-3-phosphate dehydrogenase, and cyclophilin). (See the online data supplement for details.)

Western Blot Analysis

Proteins from paired samples were processed in quadruplicate using rabbit antiactin (Sigma #A2066) and mouse anticyclic nucleotide 3' phosphodiesterase (CNP; SMI-91R, Covance) primary antibodies and IRDye 800 antirabbit and 680 antimouse (LI-COR Biosciences) secondary antibodies. Signals were simultaneously detected using the LI-COR Odyssey Infrared imaging system. CNP protein content was expressed relative to actin. (See the online data supplement for details.)

Gene Coexpression Networks

Gene coexpression networks were built through Pearson correlation of expression patterns and optimized using clustering coefficient analysis and jackknife correlation. (See the online data supplement for details.)

Results

Amygdala-Anterior Cingulate Cortex Altered Gene Expression in Human Major Depression

Large-scale gene expression profiles were generated from subdissected amygdala and anterior cingulate cortex (Figure 1A,B) in postmortem brains of male subjects with familial major depression and matched controls (Table 1). Overall correlations of gene transcript levels were significantly higher in matched pairs compared to nonmatched major depression-control pairs (Figure 1C), thus validating the pairing protocol at controlling non-disease-related factors and reducing signal variability. Three hundred ninety-five genes in anterior cingulate cortex and 191 genes in amygdala were identified by paired statistics or ANOVA models as differentially expressed in major depression (Figure S1 and 1D). A qPCR survey on adjacent tissue sections yielded highly concordant results (array-qPCR Pearson correlation $r = 0.88$, $p < e^{-5}$, $N = 16$ genes; see Figure S1 in the online data supplement and Table 3 for selected genes), confirming the sampling and technical reliability of the array data. Nevertheless, as results are expected to contain false positives, we hypothesized that identifying relevant findings within this large pool of genes would benefit from a comparison with equivalent data obtained in an animal model that recapitulates behavioral and pharmacological aspects of depression.

Profiles of Altered Gene Transcripts Are Conserved Between Human Major Depression and the UCMS Mouse Model of Depression and Are Reversed by Antidepressant Treatments in Mice

We previously reported (9) that UCMS induces a depressive-like syndrome in mice, consisting of progressive deterioration in coat state, reduced weight gain, and increased agonistic and emotion-related behaviors and that both symptom dimensions were reversed by chronic administration of an effective (fluoxetine) or putative (Crf1r antagonist) antidepressant. UCMS also induced region-specific patterns of altered gene expression in cingulate cortex and in the lateral/basolateral nuclei of the amygdala, which were reversed by both drug treatments. These behavioral and molecular results are summarized in Table 2, and the array results from that study were used here to support the analysis of the human

data. Specifically, we hypothesized that if cellular mechanisms underlying mood regulation were conserved across species, then altered transcriptome in human major depression would predict similar changes in mice after UCMS, and that the effects of antidepressants in mice would help separate the effects of major depression from those of drug exposure in humans.

We investigated the degree of conservation of altered transcript levels for ortholog genes between major depression and UCMS by analysis of directional correlations. Confirming our hypothesis, highly significant, reciprocal, and consistent predictions of molecular changes were identified in amygdala (Figures 1D and 2A). Specifically, of 191 genes with altered transcript levels in major depression, expression levels in mice were available for 105 ortholog probesets. Changes for these 105 mouse probesets were significantly correlated with human major depression-related changes ($r=0.29$, $p<0.005$). Conversely, of 299 genes with altered transcripts in amygdala of UCMS mice, the 213 identified human orthologs revealed a reciprocal mouse-to-human significant correlation of similar amplitude ($r=0.29$, $p<0.00001$). Analysis of 1,000 bootstrap resamplings demonstrated that the probability of obtaining the observed reciprocal concordance levels by chance was very low ($p<0.001$ for individual directional correlations, $p<0.001$ for concurrent positive findings in both directions). Markedly, the human-to-mouse correlations disappeared after successful antidepressant treatments in UCMS-exposed mice (Figure 2A). Thus, the pharmacological reversal of the major depression-UCMS correlation by two different antidepressants (i.e., targeting serotonergic or neuroendocrine stress pathways) demonstrated that the molecular changes supporting the major depression-UCMS correlations in amygdala were specific to the altered mood phenotype.

Toxicological screens identified the presence of antidepressants in five human subjects (four in the amygdala cohort), although these subjects were depressed at time of death, suggesting a lack of efficacy, suboptimal treatment, or treatment resistance. Similar correlations were observed between that patient subgroup and UCMS (r values ~ 0.35), thus supporting the clinical evidence of a lack of antidepressant efficacy in these subjects, at least for genes underlying the UCMS-to-major depression correlation.

Residual UCMS Effect (alr)	Neuronal/Glial Origin				Synapse Function and Development	Neurotransmission and Signaling	Cell-Matrix Interaction	Oligodendrocyte Enriched
	Log ₂ (WM/GM)	Enrichment	qPCR (p)	qPCR (alr)				
0.06	-1.9	Neuronal	0.004	0.27	X	X		
0.27	-1.6		0.070	0.49		X		
-0.08	-1.4							
0.06	-1.2		0.003	0.68	X			
0.15	-1.1						X	
0.03	-0.9		0.031	0.17		X		
-0.15	-0.9	↓	0.030	-0.58	X			
0.22	-0.7		0.060	0.39		X		
0.14	-0.6					X		
-0.05	-0.5				X			
-0.03	-0.4							
-0.15	-0.3	↓	0.090	-0.54	X			
0.08	-0.3		0.005	0.49			X	

Residual UCMS Effect (alr)	Neuronal/Glial Origin		qPCR (p)	qPCR (alr)	Synapse Function and Development	Neurotransmission and Signaling	Cell-Matrix Interaction	Oligodendrocyte Enriched
	Log ₂ (WM/GM)	Enrichment						
0.13	-0.3							
0.01	-0.2							
0.16	-0.1		0.110	0.21		X		
-0.09	-0.1	↓						
0.16	-0.1						X	
0.10	0.1					X		
-0.01	0.1							
-0.10	0.2							
-0.11	0.4	↓						
-0.33	0.6		0.001	-1.00		X		
-0.14	1.3		0.010	-0.95				X
-0.12	1.5		0.010	-0.60				X
-0.18	2.1		0.085	-0.50				X
-0.07	2.1	↓	0.080	-0.64				
0.15	2.1		0.118	-0.37				X
-0.21	2.3							X
-0.18	2.7		0.080	-0.39				X
-0.03	2.9							X
-0.10	3.1	Glial	0.019	-0.76				X

Conversely, UCMS-induced changes in mouse cingulate cortex did not predict corresponding changes in human anterior cingulate cortex ($r=0.10$), while human major-depression-related changes were also unrelated to changes in mouse cingulate cortex ($r=0.02$) (Figure 2A). These low and nonsignificant anterior cingulate cortex-cingulate cortex correlations could result from differential involvement of that brain area in major depression and UCMS, or reflect a low conservation of cingulate structure and function across species. To partly address this question, we took advantage of the robust differences in transcriptomes between anterior cingulate cortex and amygdala in human subjects (~20% of genes; >2-fold change, $p<0.01$) and between mouse cingulate cortex and amygdala (~10% of genes; >2-fold change, $p<0.01$) to estimate the degree of similarity in “molecular structure” between areas across species. We found highly significant and reciprocal correlations between human anterior cingulate cortex/amygdala and mouse cingulate cortex/amygdala differences (mouse-to-human, $r=0.63$, $p<0.0001$; human-to-mouse, $r=0.55$, $p<0.0001$). These values did not differ between major depression subjects, UCMS-treated mice, or control samples (r values ~0.60, all comparisons, not shown). These results suggested that the lack of conserved depression-related findings in anterior cingulate cortex was not due to overall differences in “molecular structures” of the amygdala/anterior cingulate cortex network across species, thus also highlighting the amygdala specificity of the human-rodent correlation of the molecular impacts of major depression and UCMS.

Amygdala Cross-Species Correlations of Depression-Related Molecular Changes Identified a Subgroup of Human Major Depression Subjects

Absent or weak mouse-human correlations in cingulate cortices could also arise from variable or opposite effects in subgroups of human subjects, resulting in a null group effect.

Indeed, despite our efforts to reduce the heterogeneity of the human cohort, major depressive disorder is by its clinical definition a heterogeneous disorder, and one may reasonably expect differences in molecular pathologies across subjects. Moreover, since the current analyses rely on large numbers of genes (178 in anterior cingulate cortex and 213 in amygdala), different gene sets may weigh differently across subjects; thus, correlation analyses in individual subjects may reveal features of cross-species predictions otherwise not available using combined group values. Here, using subjectwise changes in transcript levels for the identified genes (Figure 1D, step 3), we confirmed the lack of conserved major depression-UCMS effect in anterior cingulate cortex, as most individual human subjects displayed no cross-species correlation (Figures 1D and 2B, left panel). In amygdala, however, directional correlations revealed a large heterogeneity in cross-species predictions, with half of the subjects displaying positive correlations and the rest displaying either absent or negative correlations (Figure 2B, right panel). This difference from the anterior cingulate distribution was not explained by baseline changes, as the variability in gene expression of controls was comparable between anterior cingulate and amygdala ($p>0.2$). Rather, it was due to a selective increase in gene expression variability in the amygdala in subjects with major depression (amygdala: 50.3% higher gene transcript variance versus controls, $p<0.01$; anterior cingulate: 1% increase, $p=0.97$).

Notably, the subgroup of major depression subjects with positive UCMS correlation in amygdala (denoted here MDD_{UCMS}) did not differ in demographic parameters from controls or other subjects with major depression (all p values >0.05) and was not explained by differences in death by suicide, disease recurrence, antidepressant exposure, or alcohol dependence relative to other subjects with major depression (Figure 2B, bottom grid). The four major depression subjects with evidence of antidepressant exposure at time of death were all included in the MDD_{UCMS} subgroup, confirming the presence of a depression-related molecular profile in these subjects (i.e., positive correlation with UCMS), consistent with their clinical profile. Overall, MDD_{UCMS} subjects displayed a trend toward more depressive symptoms (7.4 versus 4.6 in the remaining major depression subjects, $p=0.07$). Interestingly, the two subjects with large negative correlations were among the only three major depression subjects who met requirements for remission or partial remission due to fewer depressive symptoms at time of death (Figure 2B, circles with red borders). Together, these findings suggest that the degree of correlation between UCMS and major depression molecular changes in amygdala may predict the severity of depression in human subjects. Indeed, a positive and significant correlation was observed between symptom numbers and UCMS-major depression correspondence ($r=0.62$, $p=0.02$; $N=14$ pairs), although this effect was partly driven by two remitted subjects (see Figure S2 in the online data supplement). Finally, restricting the analysis to MDD_{UCMS} subjects (Figure 1D, step 4), we identified a larger number of genes with altered transcript levels in amygdala ($N\approx 2,100$; 1,139 orthologs), suggesting a greater homogeneity in molecular profiles within this subgroup. In the absence of demographic identifiers, we interpreted these findings as evidence for a subgroup of major depression subjects (MDD_{UCMS}) with a consistent amygdala pathology, potentially reflecting a more severe form of the illness, and for which the UCMS rodent model provided significant predictability at the gene expression level.

Two Distinct Oligodendrocyte and Neuronal Depression-Related Phenotypes in Amygdala

To characterize putative biological events underlying the cross-species correlations of changes and to address the presence of false positives in single data sets, we focused on genes with confirmed changes across species. Selected genes had to be significantly affected by UCMS and major depression and reversed by antidepressant treatments in the mouse model (Figure 1D, step 4), thus tracking the altered mood phenotype and controlling for drug effects. Of 299 gene transcripts affected by UCMS in amygdala, 61 were also

significantly affected in major depression, mostly corresponding to changes in MDD_{UCMS} subjects. Several of these transcript changes corresponded to the same genes and were combined, reducing the selection to 44 genes. Thirty-eight of the 44 genes displayed changes in the same direction in both species. Finally, antidepressant treatments reversed changes for 32 of these genes in rodents (Table 3), together identifying a core set of genes, characterized by concordant major depression and UCMS effects and effective reversal by antidepressant treatments.

qPCR analysis on RNA extracted from adjacent tissue sections for 17 of these genes revealed a very high correlation with array results in the MDD_{UCMS} group ($r=0.95$, $p<0.00001$; Table 3), even if individual statistical significances for some genes were only at the trend level ($p=0.1$). To determine whether this represented a quantitative limitation of the qPCR assay or a lack of biological effect, we assessed changes in protein levels for CNP, one of the three genes with trend-level significance by qPCR. Quantitative Western blot analysis revealed stable CNP protein levels over the postmortem interval covered in our study (PMI/ protein, $r=0.01$; not shown), a high concordance with RNA levels ($r=0.76$ for all 14 pairs, $p=0.002$), and a significant down-regulation in MDD_{UCMS} subjects (-21.5% , $p=0.01$; Figure 3). In concert with qPCR, these findings provided supporting evidence for the technical reliability and biological validity of the identified molecular profile described in Table 3.

Within the group of genes with suggested glial enrichment of transcripts, genes were almost exclusively related to oligodendrocyte structure and function and were all down-regulated (Table 3, bottom rows). This striking convergence of gene function and direction of biological effects strongly suggests the presence of a conserved phenotype negatively affecting oligodendrocytes in amygdala under major depression and UCMS conditions. Conversely, genes with suggested neuronal enrichment of transcripts were mostly up-regulated and related to cellular maturation and synaptic development, neurotransmission and signaling, and cell-cell and cell-matrix interactions (Table 3, upper rows), suggesting a putative increase in neuronal structure and function in amygdala of major depression subjects.

Genes With Conserved Major Depression- and UCMS-Related Changes Participate in a Highly Cohesive and Interactive Gene Coexpression Network

We next investigated whether the identified genes represented various unrelated molecular findings or if they participate in shared cellular and biological functions (known as functional modules). It is possible to test these hypotheses by simultaneously inferring the interactions, or “links,” between our identified genes. These links are based on synchronized fluctuations in gene expression across samples (i.e., “coexpression” link), which have been shown to correspond to shared biological functions (30). Indeed, gene networks built on coexpression links typically cluster in functional modules that correspond to specific cellular activities (31,32), and this organization persists across species (33). Hence, biological networks built on coexpression links are a useful means of determining whether genes share common functions, and here they represent a bias-free and data-driven way to investigate putative unifying major-depression-related cellular processes shared by our identified genes.

Accordingly, we used Pearson correlations to determine pairwise coexpression links between the 32 identified genes, which were then used to build gene networks (see the online data supplement). To ensure that the coexpression links represented robust markers of biological gene interactions, we used clustering coefficient analysis and jackknife resampling methods to optimize our criteria for inclusion in the networks. Clustering coefficients estimate the density of local connections within functional modules and represent measures of network structure with wide applicability in brain networks (34).

Here, local modules were more connected than randomized networks (i.e., higher clustering coefficient; Figure 4A), indicating that the identified genes participate in shared biological functions. Pearson correlation values resulting in networks with the largest differences in clustering coefficients compared to permuted networks provide the most biological information and were retained here as optimized cutoff points to build gene networks (dashed line in Figure 4A) (35). Additionally, we used a jackknife resampling approach to remove spurious links and maximize the biological reliability of the network. The obtained bimodal distributions clearly segregated links as robust (i.e., survive jackknife resampling; Figure 4B, right bars) or spurious (i.e., do not survive jackknife; left bars) in both species. Thus, gene networks were built using 100 links from the most robust groups in the jackknife histograms (Figure 4C – D), corresponding to clustering coefficients within the suggested range of optimized values (Figure 4A; >0.65 in human; >0.75 in mouse).

The 32 identified genes formed a tightly clustered network (Figure 4C,D) with ~7 times more connections than random networks of similar size ($p < 0.01$). Moreover, the overall clustering coefficients for each network were on average 77% higher than degree-matched randomly selected reference networks ($p < 0.001$). Results were highly similar for all conditions and in both species, thus strongly supporting the biological validity and reliability of the identified network. Although the organic representation of the networks showed some differences (Figure 4C,D), the internal topology was well conserved, with a ~40% concordance of individual links across species, or ~57% using correlation of “betweenness centrality,” a more general measure of network similarity (36). Within this network, genes with suggested glial or neuronal enrichment of cellular origin of transcripts naturally segregated (Figure 4C,D), which was quantitatively reflected by higher intraconnections (glial-glial and neuronal-neuronal) than interconnections (glial-neuronal) (Figure 4E).

In summary, these results demonstrate that genes forming the identified molecular signature of depression belong to an existing and tightly connected gene network that is conserved across species and that reflects the interactive glial/neuronal cellular compartments of gray matter tissue, together suggesting an abnormal recruitment by the illness of existing cellular pathways.

Discussion

To identify the molecular pathology of major depression, a heterogeneous illness with multiple symptom dimensions, we focused on postmortem samples in a cohort with reduced clinical and demographic heterogeneity (familial major depression, male subjects) and on two brain regions (amygdala and anterior cingulate cortex) within a neural network putatively involved in altered mood regulation, a core symptom of the illness. After controlling several sources of technical variability (Figure 1) and by relying on cross-species validation and antidepressant reversal of results, we identified reciprocal predictions of altered transcriptome between major depression and the UCMS rodent model of the disease (Figure 2A). These effects were detected at the group level and also identified a subgroup of the major depression group (MDD_{UCMS}; Figure 2B) with a more homogeneous molecular pathology and for which UCMS provided a means to identify individual genes with conserved changes. Specifically, changes in transcript levels of ~30 genes were similarly detected in human major depression and mouse UCMS and were reversed by antidepressant treatments in mice, hence corresponding to a pool of genes affected in correlation with mood states. These genes belonged to an existing cohesive network (Figure 4) and suggested two distinct cellular phenotypes: decreased oligodendrocyte and up-regulated neuronal structure and function (Table 3). Finally, the interconnections between the glial and neuronal components of the network suggested either a conserved cross-talk between the two phenotypes or a common upstream mechanism. Together, the present studies confirm that

the biological liability to major depression is reflected in a persistent molecular pathology affecting the amygdala and support the hypothesis of maladaptive changes in the amygdala as a putative primary pathology in major depression.

A Phylogenetically Conserved Molecular Subtype of Depression in Amygdala

To address past difficulties, we assumed that evidence for mechanisms of mood dysregulation would manifest as weak but conserved signals between major depression and UCMS. Thus, critical analytical aspects were first to maintain a high discovery level and then to rely on cross-species validations of results, as previously described in a mouse-human comparative transcriptome study of brain aging (28). The conserved changes observed here were confirmed by permutation analyses and were of a magnitude similar to age-related changes (Pearson directional correlations of ~0.3–0.4). Thus, compared to the robust effects of aging, the molecular correlates of UCMS and major depression were surprisingly strong.

It is not known whether these conserved changes correspond to specific symptom dimensions (i.e., stress effects, or amygdala-mediated anxiety component) or to a core pathology in MDD_{UCMS} subjects, as available parameters did not correlate with the subgroup (Figure 2). Overall, MDD_{UCMS} subjects displayed more depressive symptoms at time of death. The fact that major depression subjects who met requirements for remission or partial remission displayed no correlation or a negative correlation also suggested that opposite changes may participate in both depressive and remission phenotypes. We propose that this molecular signature may represent a novel approach to categorizing major depression, based on similarities of biological changes. This molecular view of disease heterogeneity is consistent with the notion that other subjects with major depression may present altered functions in different brain regions (exerting control over the amygdala, for instance), yielding similar clinical phenotypes but through pathogenic mechanisms remote from the amygdala.

In contrast, no UCMS-major depression correlations in gene expression were identified in cingulate cortices. The complex evolutionary changes and potential differences in connectivity of this brain area may explain the lack of conserved effects, despite similarities in molecular structures. The anterior cingulate cortex integrates input from cognitive and emotion-related sources, influences activities related to decision making, and modulates neuroendocrine, motor, and visceral responses (37). Phylogenetic specializations of the human anterior cingulate include increased size, more functional subdivisions, dense prefrontal cortex connections, and cellular specializations (i.e., spindle cells) that allow distal connections with other brain regions (38,39), together reflecting the human capacity for higher integration of complex emotion and cognitive functions compared to rodents (37). Alternatively, some anterior cingulate findings may relate to the illness, but the UCMS model did not make their distinction from unrelated effects possible, as the model mimics only one of many putative pathogenic mechanisms in the illness. Hence, molecular data obtained in different models, based on cognitive- or reward-related symptoms, for instance, combined with investigations of additional brain regions, could provide additional insights on molecular dysfunctions in major depression, as different symptom dimensions likely correspond to dysfunctions in distinct neural networks (1,40). Investigating selected brain areas in human subjects, in parallel with relevant animal models of symptom dimensions, may thus represent a fruitful approach to addressing the heterogeneity of the molecular pathology of major depression. In the absence of quantitative differences in clinical features or demographic identifiers, the present findings identified a subgroup of major depression subjects (MDD_{UCMS}) with a homogeneous molecular pathology and for which UCMS provided a significant predictability at the gene expression level.

Oligodendrocyte and Principal Pyramidal Neuronal Changes in Amygdala in Depression

The striking convergence of down-regulated glial-related gene transcripts in major depression and UCMS clearly suggests a conserved phenotype selectively affecting oligodendrocytes (Table 3), consistent with reports of reduced numbers of oligodendrocytes in amygdala (19) and decreased oligodendrocyte-related gene expression in temporal cortex (4), thus establishing amygdala oligodendrocyte alterations as a confirmed pathological finding in major depression. These changes appear more robust in amygdala, since they were not observed in anterior cingulate cortex/cingulate cortex or frontal cortex (2, 3, 5, 6; see also reference 41).

The coexpression analyses revealed that the identified genes participate in a naturally occurring, tightly linked functional network that includes glial and neuronal components (Figure 4), suggesting an abnormal recruitment of existing cellular pathways, although the identity and origin of the neuronal component is not known. What mechanisms might link these two phenotypes and be informative as to their cellular characterization? Results from the network analyses suggest that the two phenotypes may occur in concert, either through mutual interactions or downstream from a common perturbation. We speculate that the converging effects of increased amygdala recruitment (e.g., through excitatory glutamatergic neurotransmission originating from stress-related sensorimotor modalities) and elevated stress-induced glucocorticoid exposure, such as occurs in UCMS and has been suggested in major depression, may provide a common synergistic mechanism.

Both effects would be consistent with the observed glial phenotype, in view of the known vulnerability of oligodendrocytes to glutamatergic excitotoxicity (42) and inhibitory effect of glucocorticoids on oligodendrocyte proliferation (43,44). Accordingly, decreased oligodendrocyte gene transcripts may represent early evidence of combined excitotoxic insults and glucocorticoid inhibition, leading over time to decreased oligodendrocyte numbers in major depression (19).

On the other hand, this putative synergistic mechanism would suggest amygdala principal pyramidal cells as the likely source of the neuronal molecular pathology. Indeed, the convergence of increased ARHGAP6 (a RhoA inhibitor), CACNB2 (voltage-dependent calcium channel), and modulators of glutamatergic synaptic plasticity (CAMK2D, EGR1), coupled with increased components of cell-matrix remodeling (MATN2, CDH13, and CHSY1), suggest increased structural and functional dendritic/synaptic compartments. This interpretation is consistent with the reported increased dendritic branching in pyramidal neurons in the rat amygdala after chronic mild stress (45) and with the increased excitability of amygdala basolateral pyramidal neurons after glucocorticoid exposure (46). Together with the absence of changes of interneuron markers, the known stimulatory effect of glucocorticoids on amygdala principal cells (46), and an expected activity-driven dendritic structural up-regulation, the present results suggest an increased structure/function phenotype of amygdala principal pyramidal cells in UCMS and major depression. In humans, these proposed neuronal changes may correspond to cellular and molecular correlates of increased amygdala function in major depression (20,21,47), although the causes may be complex and combine adaptive (or maladaptive) mechanisms and intrinsic genetic vulnerability (10,48).

These results await replication in independent cohorts. The scarcity of well-characterized human postmortem brains of male subjects with familial major depression prevented the direct replication in our brain bank, and it is not known whether different demographic and clinical parameters (e.g., female subjects, nonfamilial depression) will affect the nature and/or robustness of the molecular findings. Another limitation concerns the presence of antidepressant treatments. In this study, antidepressant-treated subjects still met DSM-IV

criteria for major depressive disorder, which suggests lack of efficacy, consistent with molecular profiles suggesting depressive-like states. Finally, numerous additional genes were identified, but the putative association of these genes with major depression could not be confirmed in the absence of independent cohorts or of animal models for alternative pathogenic mechanisms in the illness.

Supplementary Material

Refer to Web version on PubMed Central for supplementary material.

Acknowledgments

Supported by NIMH grants MH067721 and MH077159 (to Dr. Sibille) and grant MH45156 (to Dr. Lewis) and by a fellowship from the University of Pittsburgh Institute for Clinical Research Education and Clinical and Translational Science (to Mr. Gaiteri). The funding agency had no role in the study design, data collection and analysis, decision to publish, and preparation of the manuscript. The content is solely the responsibility of the authors and does not necessarily represent the official views of NIMH or NIH.

The authors thank Jean-Philippe Guilloux, Ph.D., for his expertise in quantitative polymerase chain reaction.

References

1. Belmaker RH, Agam G. Major depressive disorder. *N Engl J Med* 2008;358:55–68. [PubMed: 18172175]
2. Sibille E, Arango V, Galfalvy HC, Pavlidis P, Erraji-BenChekroun L, Ellis SP, Mann JJ. Gene expression profiling of depression and suicide in human prefrontal cortex. *Neuropsychopharmacology* 2004;29:351–361. [PubMed: 14603265]
3. Choudary PV, Molnar M, Evans SJ, Tomita H, Li JZ, Vawter MP, Myers RM, Bunney WE Jr, Akil H, Watson SJ, Jones EG. Altered cortical glutamatergic and GABAergic signal transmission with glial involvement in depression. *Proc Natl Acad Sci USA* 2005;102:15653–15658. [PubMed: 16230605]
4. Aston C, Jiang L, Sokolov BP. Transcriptional profiling reveals evidence for signaling and oligodendroglial abnormalities in the temporal cortex from patients with major depressive disorder. *Mol Psychiatry* 2005;10:309–322. [PubMed: 15303102]
5. Sequeira A, Gwadry FG, Ffrench-Mullen JM, Canetti L, Gingras Y, Casero RA Jr, Rouleau G, Benkelfat C, Turecki G. Implication of SSAT by gene expression and genetic variation in suicide and major depression. *Arch Gen Psychiatry* 2006;63:35–48. [PubMed: 16389195]
6. Kang HJ, Adams DH, Simen A, Simen BB, Rajkowska G, Stock-meier CA, Overholser JC, Meltzer HY, Jurjus GJ, Konick LC, Newton SS, Duman RS. Gene expression profiling in postmortem prefrontal cortex of major depressive disorder. *J Neurosci* 2007;27:13329–13340. [PubMed: 18045927]
7. Hasler G, Drevets WC, Manji HK, Charney DS. Discovering endophenotypes for major depression. *Neuropsychopharmacology* 2004;29:1765–1781. [PubMed: 15213704]
8. Willner P. Chronic mild stress (CMS) revisited: consistency and behavioural-neurobiological concordance in the effects of CMS. *Neuropsychobiology* 2005;52:90–110. [PubMed: 16037678]
9. Surget A, Wang Y, Leman S, Ibarguen-Vargas Y, Edgar N, Griebel G, Belzung C, Sibille E. Corticolimbic transcriptome changes are state-dependent and region-specific in a rodent model of depression and of antidepressant reversal. *Neuropsychopharmacology* 2009;34:1363–1380. [PubMed: 18536703]
10. Pezawas L, Meyer-Lindenberg A, Drabant EM, Verchinski BA, Munoz KE, Kolachana BS, Egan MF, Mattay VS, Hariri AR, Weinberger DR. 5-HTTLPR polymorphism impacts human cingulate-amygdala interactions: a genetic susceptibility mechanism for depression. *Nat Neurosci* 2005;8:828–834. [PubMed: 15880108]

11. Seminowicz DA, Mayberg HS, McIntosh AR, Goldapple K, Kennedy S, Segal Z, Rafi-Tari S. Limbic-frontal circuitry in major depression: a path modeling metanalysis. *Neuroimage* 2004;22:409–418. [PubMed: 15110034]
12. Drevets WC, Price JL, Simpson JR Jr, Todd RD, Reich T, Vannier M, Raichle ME. Subgenual prefrontal cortex abnormalities in mood disorders. *Nature* 1997;386:824–827. [PubMed: 9126739]
13. Botteron KN, Raichle ME, Drevets WC, Heath AC, Todd RD. Volumetric reduction in left subgenual prefrontal cortex in early onset depression. *Biol Psychiatry* 2002;51:342–344. [PubMed: 11958786]
14. Mayberg HS, Liotti M, Brannan SK, McGinnis S, Mahurin RK, Jerabek PA, Silva JA, Tekell JL, Martin CC, Lancaster JL, Fox PT. Reciprocal limbic-cortical function and negative mood: converging PET findings in depression and normal sadness. *Am J Psychiatry* 1999;156:675–682. [PubMed: 10327898]
15. Drevets WC, Bogers W, Raichle ME. Functional anatomical correlates of antidepressant drug treatment assessed using PET measures of regional glucose metabolism. *Eur Neuropsychopharmacol* 2002;12:527–544. [PubMed: 12468016]
16. Cotter D, Mackay D, Landau S, Kerwin R, Everall I. Reduced glial cell density and neuronal size in the anterior cingulate cortex in major depressive disorder. *Arch Gen Psychiatry* 2001;58:545–553. [PubMed: 11386983]
17. Ongur D, Drevets WC, Price JL. Glial reduction in the subgenual prefrontal cortex in mood disorders. *Proc Natl Acad Sci USA* 1998;95:13290–13295. [PubMed: 9789081]
18. Bowley MP, Drevets WC, Ongur D, Price JL. Low glial numbers in the amygdala in major depressive disorder. *Biol Psychiatry* 2002;52:404–412. [PubMed: 12242056]
19. Hamidi M, Drevets WC, Price JL. Glial reduction in amygdala in major depressive disorder is due to oligodendrocytes. *Biol Psychiatry* 2004;55:563–569. [PubMed: 15013824]
20. Sheline YI, Barch DM, Donnelly JM, Ollinger JM, Snyder AZ, Mintun MA. Increased amygdala response to masked emotional faces in depressed subjects resolves with antidepressant treatment: an fMRI study. *Biol Psychiatry* 2001;50:651–658. [PubMed: 11704071]
21. Siegle GJ, Steinhauer SR, Thase ME, Stenger VA, Carter CS. Can't shake that feeling: event-related fMRI assessment of sustained amygdala activity in response to emotional information in depressed individuals. *Biol Psychiatry* 2002;51:693–707. [PubMed: 11983183]
22. Roberson-Nay R, McClure EB, Monk CS, Nelson EE, Guyer AE, Fromm SJ, Charney DS, Leibenluft E, Blair J, Ernst M, Pine DS. Increased amygdala activity during successful memory encoding in adolescent major depressive disorder: an fMRI study. *Biol Psychiatry* 2006;60:966–973. [PubMed: 16603133]
23. Sibille E, Arango V, Joeyen-Waldorf J, Wang Y, Leman S, Surget A, Belzung C, Mann JJ, Lewis DA. Large-scale estimates of cellular origins of mRNAs: enhancing the yield of transcriptome analyses. *J Neurosci Methods* 2008;167:198–206. [PubMed: 17889939]
24. Irizarry RA, Bolstad BM, Collin F, Cope LM, Hobbs B, Speed TP. Summaries of Affymetrix GeneChip probe level data. *Nucleic Acids Res* 2003;31:e15. [PubMed: 12582260]
25. Santarelli L, Saxe M, Gross C, Surget A, Battaglia F, Dulawa S, Weisstaub N, Lee J, Duman R, Arancio O, Belzung C, Hen R. Requirement of hippocampal neurogenesis for the behavioral effects of antidepressants. *Science* 2003;301:805–809. [PubMed: 12907793]
26. Bodnoff SR, Suranyi-Cadotte B, Aitken DH, Quirion R, Meaney MJ. The effects of chronic antidepressant treatment in an animal model of anxiety. *Psychopharmacology (Berl)* 1988;95:298–302. [PubMed: 3137614]
27. Mineur YS, Prasol DJ, Belzung C, Crusio WE. Agonistic behavior and unpredictable chronic mild stress in mice. *Behav Genet* 2003;33:513–519. [PubMed: 14574128]
28. Sibille E, Su J, Leman S, Le Guisquet AM, Ibarguen-Vargas Y, Joeyen-Waldorf J, Glorioso C, Tseng GC, Pezzone M, Hen R, Belzung C. Lack of serotonin(1B) receptor expression leads to age-related motor dysfunction, early onset of brain molecular aging, and reduced longevity. *Mol Psychiatry* 2007;12:1042–1056. [PubMed: 17420766]
29. Akaike H. A new look at the statistical model identification. *IEEE Transact Automatic Control* 1974;19:716–723.

30. Lee HK, Hsu AK, Sajdak J, Qin J, Pavlidis P. Coexpression analysis of human genes across many microarray data sets. *Genome Res* 2003;14:1085–1094. [PubMed: 15173114]
31. Zhang B, Horvath S. A general framework for weighted gene co-expression network analysis. *Stat Appl Genet Mol Biol* 2005;4(1)
32. Oldham MC, Konopka G, Iwamoto K, Langfelder P, Kato T, Horvath S, Geschwind DH. Functional organization of the transcriptome in human brain. *Nat Neurosci* 2008;11:1271–1282. [PubMed: 18849986]
33. Bergmann S, Ihmels J, Barkai N. Similarities and differences in genome-wide expression data of six organisms. *PLoS Biol* 2004;2:E9. [PubMed: 14737187]
34. Sporns O, Chialvo DR, Kaiser M, Hilgetag CC. Organization development and function of complex brain networks. *Trends Cogn Sci* 2004;8:418–425. [PubMed: 15350243]
35. Elo LL, Jarvenpaa H, Oresic M, Lahesmaa R, Aittokallio T. Systematic construction of gene coexpression networks with applications to human T helper cell differentiation process. *Bioinformatics* 2007;23:2096–2103. [PubMed: 17553854]
36. Girvan M, Newman ME. Community structure in social and biological networks. *Proc Natl Acad Sci USA* 2002;99:7821–7826. [PubMed: 12060727]
37. Paus T. Primate anterior cingulate cortex: where motor control, drive, and cognition interface. *Nat Rev Neurosci* 2001;2:417–424. [PubMed: 11389475]
38. Allman JM, Hakeem A, Erwin JM, Nimchinsky E, Hof P. The anterior cingulate cortex: the evolution of an interface between emotion and cognition. *Ann NY Acad Sci* 2001;935:107–117. [PubMed: 11411161]
39. Allman J, Hakeem A, Watson K. Two phylogenetic specializations in the human brain. *Neuroscientist* 2002;8:335–346. [PubMed: 12194502]
40. Nestler EJ, Barrot M, DiLeone RJ, Eisch AJ, Gold SJ, Monteggia LM. Neurobiology of depression. *Neuron* 2002;34:13–25. [PubMed: 11931738]
41. Uranova NA, Vostrikov VM, Orlovskaya DD, Rachmanova VI. Oligodendroglial density in the prefrontal cortex in schizophrenia and mood disorders: a study from the Stanley Neuropathology Consortium. *Schizophr Res* 2004;67:269–275. [PubMed: 14984887]
42. Rosin C, Bates TE, Skaper SD. Excitatory amino acid induced oligodendrocyte cell death in vitro: receptor-dependent and -independent mechanisms. *J Neurochem* 2004;90:1173–1185. [PubMed: 15312172]
43. Banasr M, Valentine GW, Li XY, Gourley SL, Taylor JR, Duman RS. Chronic unpredictable stress decreases cell proliferation in the cerebral cortex of the adult rat. *Biol Psychiatry* 2007;62:496–504. [PubMed: 17585885]
44. Wennstrom M, Hellsten J, Ekstrand J, Lindgren H, Tingstrom A. Corticosterone-induced inhibition of gliogenesis in rat hippocampus is counteracted by electroconvulsive seizures. *Biol Psychiatry* 2006;59:178–186. [PubMed: 16431219]
45. Vyas A, Mitra R, Shankaranarayana Rao BS, Chattarji S. Chronic stress induces contrasting patterns of dendritic remodeling in hippocampal and amygdaloid neurons. *J Neurosci* 2002;22:6810–6818. [PubMed: 12151561]
46. Duvarci S, Pare D. Glucocorticoids enhance the excitability of principal basolateral amygdala neurons. *J Neurosci* 2007;27:4482–4491. [PubMed: 17442833]
47. Drevets WC. Prefrontal cortical-amygdalar metabolism in major depression. *Ann NY Acad Sci* 1999;877:614–637. [PubMed: 10415674]
48. Hariri AR, Mattay VS, Tessitore A, Kolachana B, Fera F, Goldman D, Egan MF, Weinberger DR. Serotonin transporter genetic variation and the response of the human amygdala. *Science* 2002;297:400–403. [PubMed: 12130784]

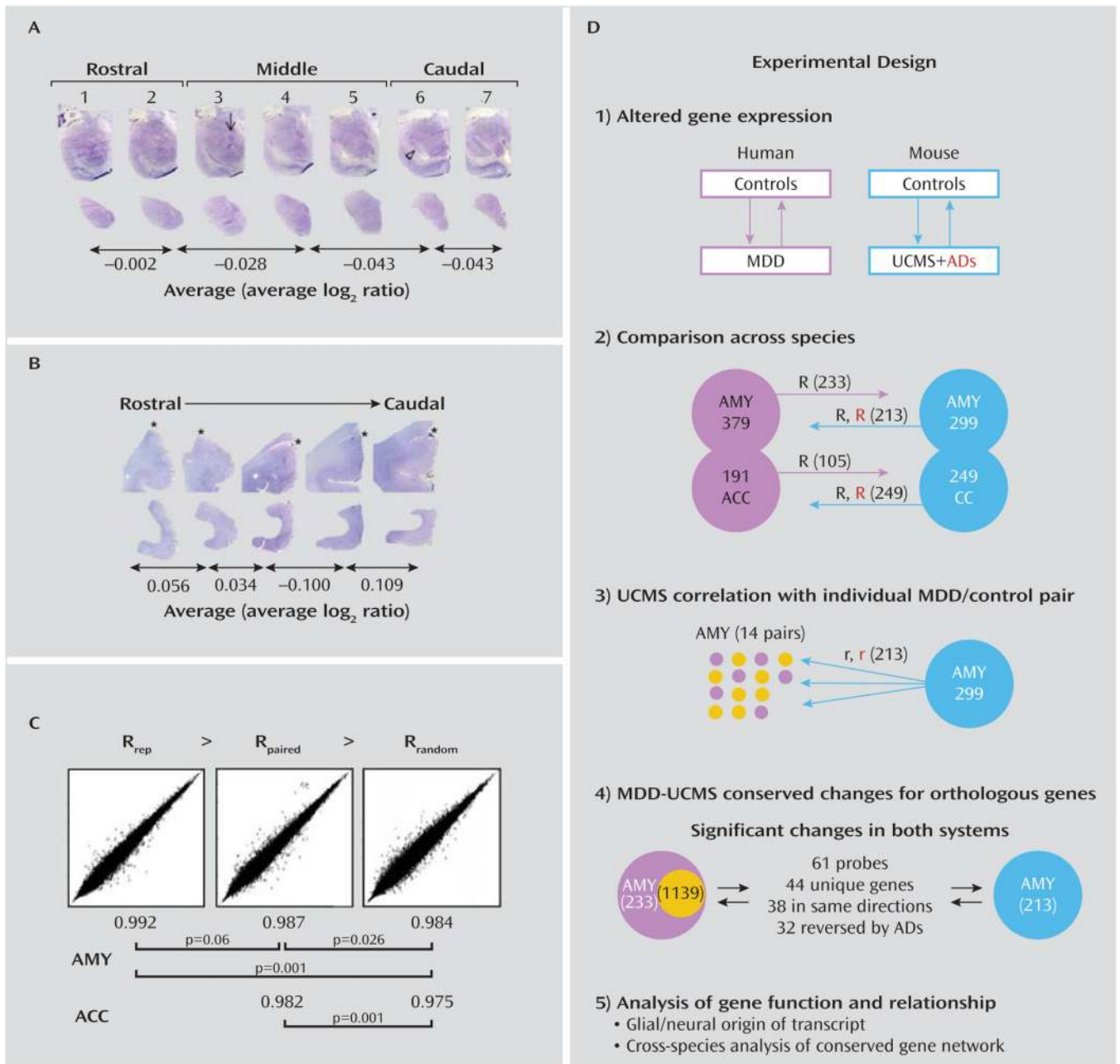


FIGURE 1. Amygdala and Anterior Cingulate Cortex Sampling Pilot Study, Effect of Pairing Protocol on Analytical Sensitivity, and Outline of Experimental Design

^a In panel A, amygdala microdissected samples (bottom) from serial 20- μ m sections 1 mm apart were processed on microarrays along the rostral-caudal axis for sections 1, 2, 4, 6, and 7. Markers for the middle and caudal amygdala were the dorsolateral subnuclei of the basolateral nucleus (arrow) and the appearance of the hippocampus (arrowhead). The lowest variability was observed between levels 1 and 2, as indicated by the average changes for detected genes (average \log_2 ratio). In panel B, 20- μ m serial sections through the rostral subgenual anterior cingulate cortex were initiated with the rostral tip of the subgenual anterior cingulate cortex. Asterisks indicate the boundary between anterior cingulate cortex and corpus callosum. Microarray samples were processed on the gray matter from five subdivided sections 1 mm apart (bottom). Although absolute values were generally higher

than in amygdala, the lowest average variability in transcript levels was detected between levels 1 and 2 in rostral anterior cingulate cortex. Accordingly, sampling was performed for all subjects at the levels of sections 1 and 2 in amygdala and anterior cingulate cortex. In panel C, representative log₂-based correlation graphs for all detected transcripts illustrate the effect of the pairing protocol on reducing non-disease-related effects. “R” stands for Pearson correlation factor. “Rep” indicates technical replicates. “Random” indicates non-paired major depression and control samples. Below the graphs, p values are from exact Wilcoxon signed-ranks test performed on ~26,000 gene transcripts with detectable levels. Panel D summarizes the experimental design. After 1) analyses of altered gene expression in major depression and UCMS, 2) the degree to which changes in one species predicted similar trends at the group level in the other species was assessed. Next, 3) UCMS predictions of gene changes in individual subjects with major depression were assessed. Then, 4) individual genes with conserved changes and antidepressant reversal were selected between UCMS and all major depression subjects (violet and yellow circles) or those with the subgroup of major depression subjects with positive UCMS correlation in amygdala (MDD_{UCMS} subgroup, yellow circles), and 5) assessed for known cellular origin, function, and relationship. R indicates the directional Pearson correlation coefficient, including after antidepressant treatments (in red). Values not in parentheses in steps 2, 3, and 4 indicate genes with significant effects in step 1; values in parentheses indicate the numbers of identified mouse-human orthologs among significant genes that were used for cross-species analyses. AMY=amygdala; ACC=anterior cingulate cortex; CC=cingulate cortex; MDD=major depressive disorder; UCMS=unpredictable chronic mild stress rodent model; ADs=antidepressants.

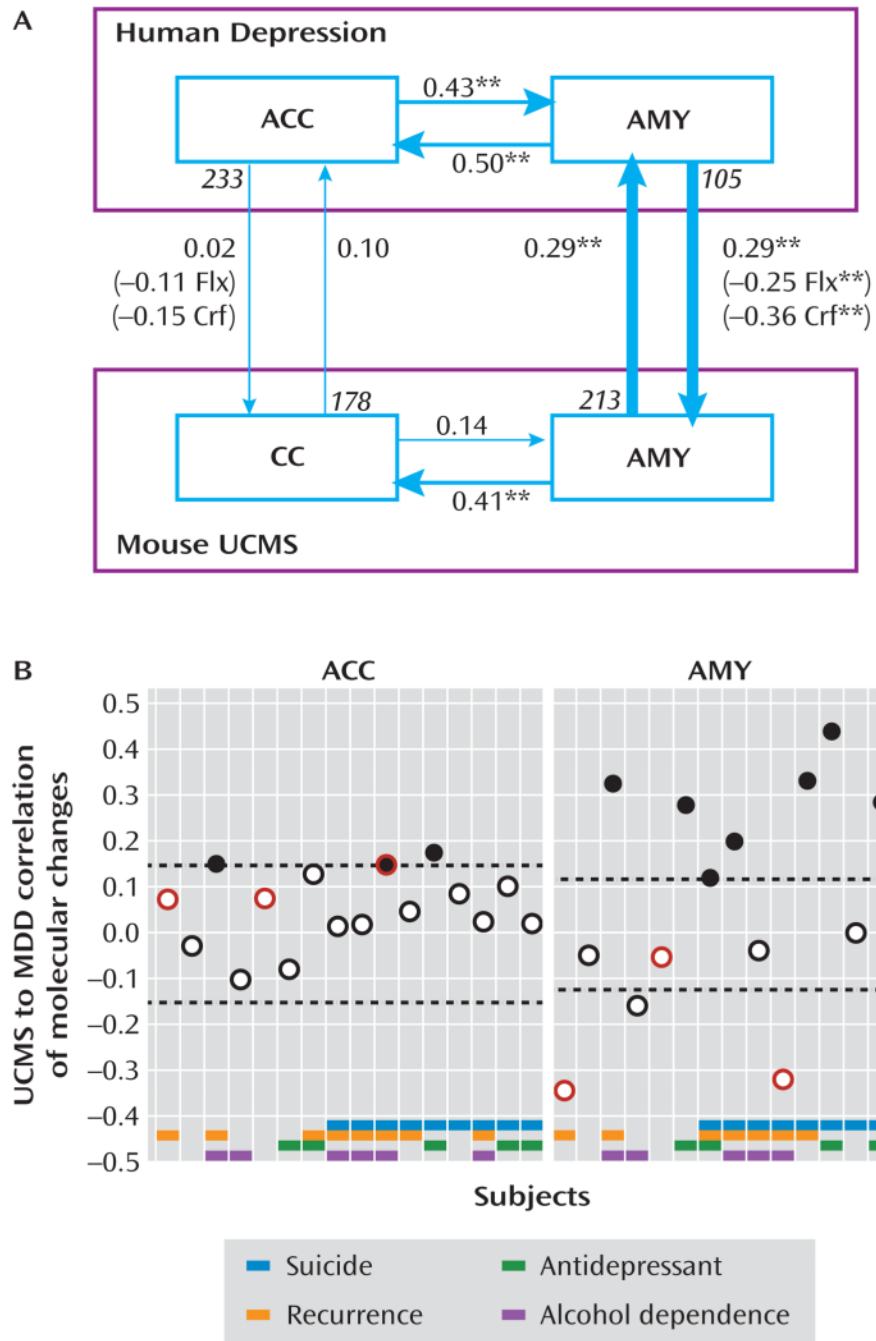


FIGURE 2. Reciprocal Prediction of Altered Amygdala Gene Expression Between Human Major Depression and the Mouse UCMS Model of Depression, and Reversal by Antidepressant Drug Treatments^a

^a In panel A, arrows indicate directional correlations between changes in transcript levels for genes identified in one area (origin of arrow) and changes for the same genes across areas within species, or within the same areas but across species (end of arrow). Numbers at the origin of the vertical arrows indicate the numbers of genes significantly affected in that species and for which data were available for orthologous genes in the other species. Averaged group values per gene transcript were used here when assessing major depression-UCMS correlation. Numbers in parentheses indicate levels of directional correlations

between human major depression and UCMS-exposed mice chronically treated with two anti-depressants (Flx=fluoxetine; Crf=Crf1r antagonist), and asterisks indicate significance (** $p < 0.001$). In panel B, correlation between UCMS and individual major depression subjects confirmed the absence of conserved effect in anterior cingulate cortex and identified a subgroup of major depression subjects with significant and positive cross-species correlations of altered transcript levels in the amygdala. Subjectwise gene transcript changes were used here. Black dots indicate significant positive correlation. Red borders indicate subjects under partial or full remission at time of death. Dashed lines represent boundaries for significance of correlations. AMY=amygdala; ACC=anterior cingulate cortex; CC=cingulate cortex; MDD=major depressive disorder; UCMS=unpredictable chronic mild stress rodent model.

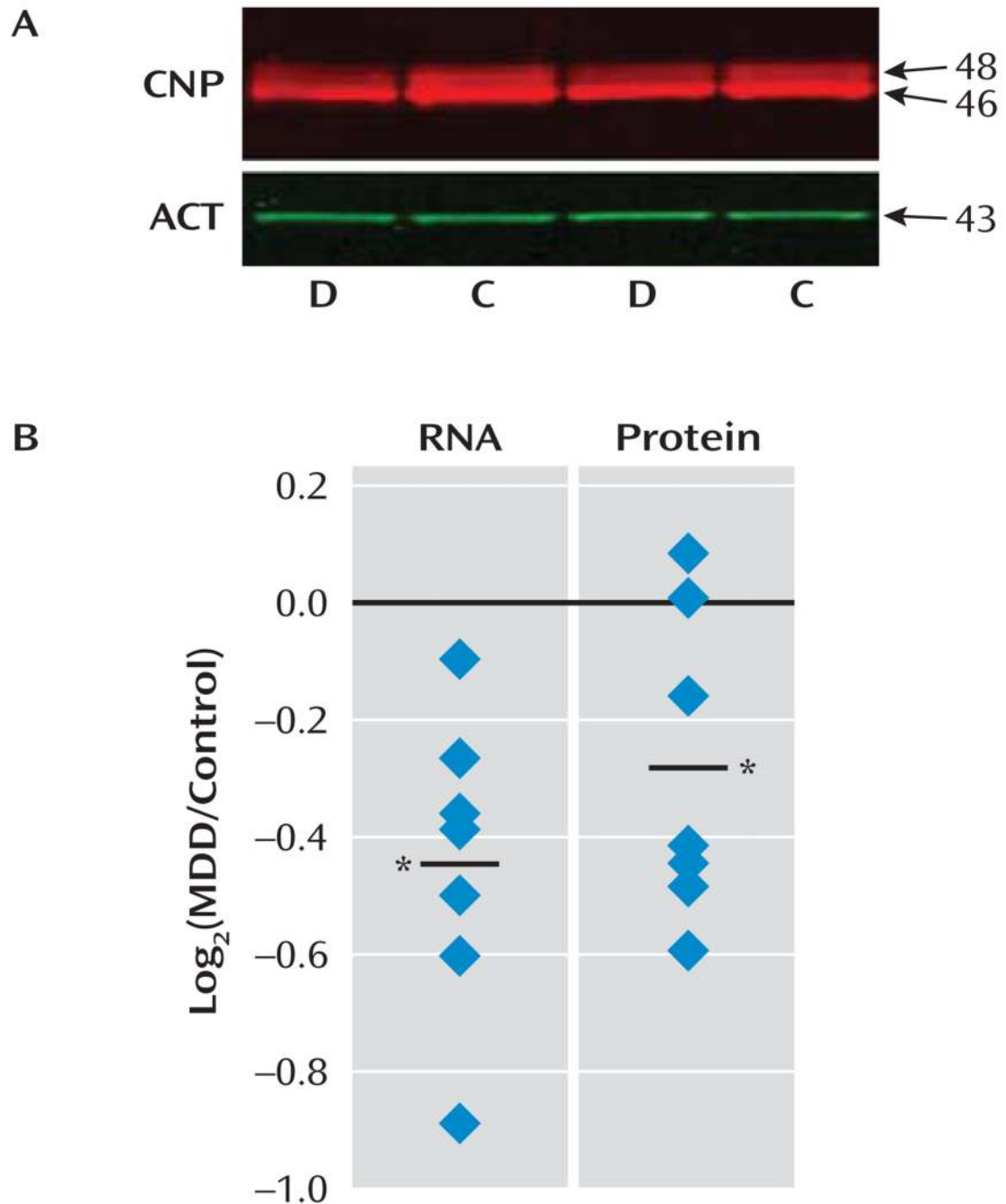


FIGURE 3. Concordant CNP RNA and Protein Down-Regulation in MDD_{UCMS} Subjects^a

^a Western blot analysis (panel A) revealed the expected bands for the two CNP protein isoforms. D and C indicate replicate major depression and control samples from the same matched pair of subjects. Panel B shows a quantitative plot denoting significant *CNP* down-regulation at the RNA (-29.2%, $p < 0.01$; array results) and protein (-21.5%, $p = 0.01$) levels in MDD_{UCMS} subjects. Both protein isoforms were similarly affected.

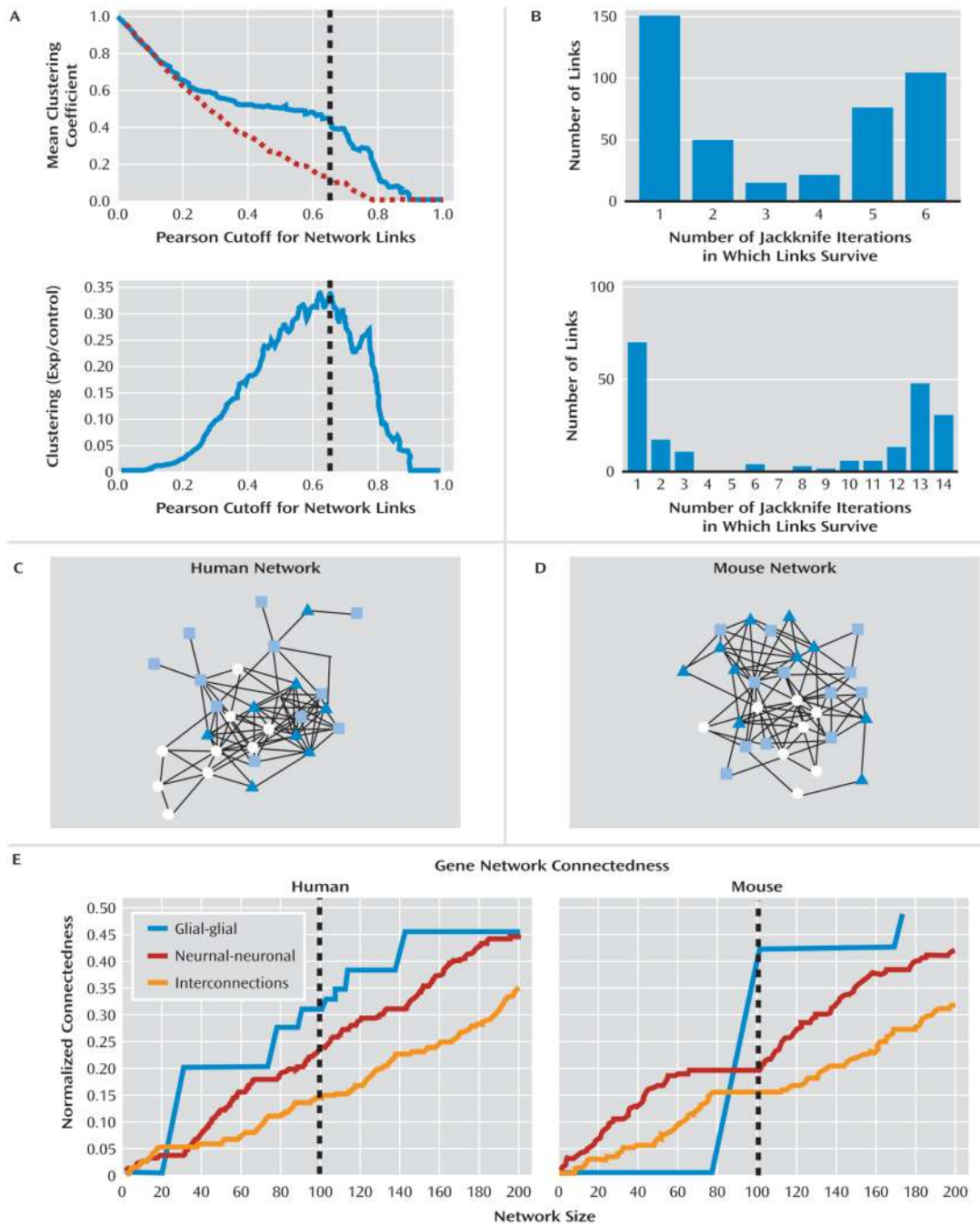


FIGURE 4. A Conserved and Tightly Clustered Gene Coexpression Network With Distinct Glial and Neuronal Components Underlies the Identified Molecular Signature of Depression^a

^a Panels A and B show optimized parameters for building gene coexpression networks. In the top graph of panel A, the mean clustering coefficient for permuted degree-matched control networks decreases monotonically (dashed line). However, clustering in experimental networks showed a relative increase compared to permuted values at cutoff values in the region of 0.5–0.8 for both human (shown) and mouse (not shown) networks, indicating biologically relevant network structure (35). In the bottom graph, optimum Pearson correlation cutoffs for mean clustering coefficients (dashed line) were estimated by subtracting values of permuted degree-matched networks from actual values.

Representative plots are from human control subjects. In panel B, the histograms of link robustness under jackknife correlation demonstrated the common bimodal distributions between robust (right bars) and spurious (left bars) links in human (bottom) and mouse (top) networks. Panels C and D shown an organic representation of the coexpression networks formed by genes supporting the molecular signature of depression in humans and mice, based on parameters optimized in panels A and B. White circles indicate glial-enriched gene transcripts; light to dark blue shapes indicate genes with increasing enrichment in neuronal origin of transcripts. Links between nodes represent coexpression links. Panel E shows plots of glial-glial, neuronal-neuronal, and neuronal-glial connectedness (i.e., number of connections within groups of genes divided by the total number of possible connections between those genes) as a function of network sizes (i.e., number of links). The visual segregation of glial-enriched and neuronal-enriched genes observed in panels C and D was reflected by increased numbers of connections within glial or neuronal groups compared to glial-neuronal connections (i.e., vertical distances for given network sizes). The sudden emergence of glial networks reflects the modularity of coexpression networks formed by fewer genes (and fewer samples in the mouse study) and is a strong indicator of unified function. The vertical dashed lines represent the chosen optimized cutoffs for network design using robust parameters from A to B and inclusion of representative glial-glial, neuronal-neuronal, and neuronal-glial connectedness.

TABLE 1
Major Depression and Control Cohorts in a Gene Expression Study of Depression

Pair	Case	Age (Years)	Postmortem Interval (Hours)		pH	Storage ^a (Months)	RNA Integrity Number	Major Depression Group			
			Age (Years)	Interval (Hours)				Suicide	Recurrent Episode	Antidepressant at Death	Alcohol Dependence at Death
1	505	57	12.8	7.1	7.1	125	8.7	Y	Y	N	Y
2	513	25	13.1	6.9	6.9	123	7.0	Y	Y	N	N
3	598	69	5.9	7.3	7.3	111	8.8	Y	N	Y	N
4	600	64	9.9	6.7	6.7	110	7.1	Y	N	N	N
5 ^b	613	59	15.6	7.0	7.0	108	8.7	Y	Y	N	Y
6 ^b	619	55	18.8	6.9	6.9	107	7.9	Y	N	Y	N
7	698	59	13.0	6.8	6.8	96	9.0	Y	N	Y	N
8	783	63	11.5	6.5	6.5	82	8.8	N	Y	N	N
9	863	52	28.3	7.2	7.2	65	8.4	N	N	N	N
10	868	47	10.5	6.8	6.8	64	8.1	N	Y	N	Y
11	926	57	19.0	7.0	7.0	20	7.3	N	N	N	Y
12	1001	54	7.3	6.6	6.6	67	7.6	N	N	N	N
13	1049	48	5.4	6.6	6.6	30	8.4	N	N	Y	N
14	809	50	20.0	6.9	6.9	77	8.5	N	Y	Y	N
15	1060	30	11.1	6.6	6.6	97	8.3	Y	Y	N	Y
16	943	56	15.4	6.6	6.6	26	8.2	Y	Y	N	Y
Amygdala											
Mean or %	52.4	13.1	6.8	77.9	8.2	50%	50%	29%	36%		
SD	12.3	6.2	0.2	35.6	0.6						
ACC ^c											
Mean or %	53.0	13.6	6.8	81.6	8.2	56%	50%	31%	38%		
SD	12.3	6.1	0.2	35.0	0.7						

^aFreezer storage at -80°C.

^b Samples from pairs 5 and 6 were not available in amygdala; thus, group parameters were compared separately for 16 pairs in anterior cingulate cortex and 14 pairs in amygdala. Average values for age, postmortem interval, pH, storage time, and RNA quality were not different between major depression and control groups.

^c Anterior cingulate cortex.

TABLE 2
 Summary of Physical and Behavioral Changes Evoked in the UCMS Mouse Model of Depression, and Reversal by Chronic Exposure to Two Antidepressant Treatments^a

Animal Group	Physical Effects		Emotion-Related Behavior		Altered Gene Expression	
	Body Weight	Fur Coat Quality	Anxiety-Like	Agonistic	Cingulate Cortex	Amygdala
Control animals	Increased ^b	No change	Not applicable	Not applicable	Not applicable	Not applicable
UCMS group	Smaller increase ^c	Decreased ^c	Increased ^c	Increased ^c	254 genes	299 genes
UCMS + fluoxetine group	Reversed ^b	Reversed ^b	Reversed ^b	Reversed ^b	75% reversal	72% reversal
UCMS + Crf1r group	Reversed ^b	Reversed ^b	Reversed ^b	Reversed ^b	44% reversal	77% reversal

^aUCMS=unpredictable chronic mild stress rodent model; Crf1r=corticotropin-releasing factor receptor 1 antagonist, SSR125543. Data are from Surget et al. (9). The physical effects, emotion-related changes, and associated gene changes evoked by UCMS were reversed by chronic anti-depressant exposure. Behavior: N=18–19 per group; array: N=6 arrays per group; statistical criteria, analysis of variance $p < 0.05$, group differences $> 20\%$.

^bSignificant effect of antidepressant reversal.

^cSignificant effect of UCMS.

TABLE 3
Core Genes Significantly Affected in Human Major Depression and Mouse UCMS

Gene Title	Gene Symbol	Entrez Gene	Human MDD		Mouse UCMS			
			All MDD Subjects (n)	MDD _{UCMS} Subjects (n)	UCMS Effect (air)	Fk Reversal (%)	Residual UCMS Effect (air)	CrfIr Reversal (%)
Calcium channel, voltage-dependent, beta 2 subunit ^b	CACNB2	783	0.02	0.49	0.37	91	0.03	84
Calcium/calmodulin-dependent protein kinase II delta	CAMK2D	817	0.08	1.07	0.54	51	0.27	50
Ankyrin repeat domain 43	ANKRD43	134548	0.06	0.28	0.44	107	-0.03	119
Rho GTPase activating protein 6	ARHGAP6	395	0.42	0.75	0.45	151	-0.23	87
Cadherin 13, H-cadherin (heart)	CDH13	1012	0.18	0.42	0.45	84	0.07	66
Dialcylglycerol kinase, gamma 90kDa	DGKG	1608	0.34	0.44	0.46	151	-0.23	93
Early growth response 1	EGR1	1958	-0.29	-0.30	-0.29	48	-0.15	50
Neuronal pentraxin I	NPTX1	4884	0.10	0.35	0.35	99	0.00	38
V-jun sarcoma virus 17 oncogene homolog ^b	JUN	3725	0.19	0.66	0.39	98	0.01	64
Protein phosphatase 1, regulatory (inhibitor) subunit 16A	PPP1R16A	84988	-0.01	-0.23	-0.27	70	-0.08	83
Transmembrane protein 17	TMEM17	200728	0.09	0.26	0.37	91	0.03	109
Rabphilin 3A homolog	RPH3A	22895	-0.36	-0.47	-0.33	82	-0.06	53
Matrilin 2	MATN2	4147	0.33	0.64	0.80	111	-0.09	90
Zinc finger protein 703	ZNF703	80139	-0.09	-0.24	-0.33	66	-0.11	140
Chromosome 5 open reading frame 22	C5orf22	55322	0.02	0.60	0.34	88	0.04	98
Potassium channel tetramerisation domain containing 12 ^b	KCTD12	115207	0.17	0.34	0.31	127	-0.09	49
P18SRP protein ^b	P18SRP	285672	0.05	0.45	0.27	96	0.01	134
Carbohydrate (chondroitin) synthase 1	CHSY1	22856	0.02	0.30	0.30	50	0.15	46
Nuclear factor I/B	NFIB	4781	0.08	0.41	0.50	153	-0.27	80
Integral membrane protein 2A ^b	ITM2A	9452	-0.15	-0.41	-0.35	114	0.05	96
Chromosome 5 open reading frame 13	C5orf13	9315	-0.16	-0.45	-0.46	111	0.05	78
Zinc finger protein, multitype 1	ZFPM1	161882	0.0	-0.25	-0.58	62	-0.22	81
Copine family member IX	CPNE9	151835	-0.29	-0.65	-0.70	52	-0.34	53
Myelin basic protein ^b	MBP	4155	-0.22	-0.41	-0.51	72	-0.14	73
Aspartylglucosaminidase	AGA	175	-0.26	-0.19	-0.38	112	0.05	69

Gene Title	Gene Symbol	Entrez Gene	Human MDD			Mouse UCMS		
			All MDD Subjects (alr)	MDD _{UCMS} Subjects (alr)	UCMS Effect (alr)	Flx Reversal (%)	Residual UCMS Effect (alr)	CrfIr Reversal (%)
2',3'-cyclic nucleotide 3'-phosphodiesterase ^b	CNP	1267	-0.12	-0.37	-0.56	58	-0.24	68
Breast carcinoma amplified sequence 1	BCAS1	8537	0.02	-0.41	-0.65	82	-0.12	89
Ectonucleotide pyrophosphatase/phosphodiesterase 2 ^b	ENPP2	5168	-0.12	-0.29	-0.50	107	0.04	130
Plasma membrane proteolipid (plasmalipin)	PLLP	51090	-0.16	-0.40	-0.56	46	-0.30	62
Endothelial differentiation, lysosphosphatidic acid GPCR 2 ^b	EDG2	1902	-0.10	-0.40	-0.85	61	-0.33	79
G protein-coupled receptor 37	GPR37	2861	-0.31	-0.52	-0.50	69	-0.16	95
Myelin-associated oligodendrocyte basic protein	MOBP	4336	-0.11	-0.51	-0.88	83	-0.15	88

^a MDD=major depressive disorder; UCMS=unpredictable chronic mild stress rodent model; Flx=fluoxetine; CrfIr=corticotropin-releasing factor receptor 1 antagonist; qPCR=quantitative polymerase chain reaction. Red shading indicates significant up-regulation, blue shading indicates significant down-regulation. Reversal percentages indicate the degree to which the drug treatments opposed the UCMS effect and brought transcript levels (alr=average log₂ ratio) back to control levels. "Residual effect" indicates changes in gene transcripts after antidepressant treatments in UCMS-exposed mice. "Log₂(WM/GM)" indicates relative glial (high LogR, bottom rows) to neuronal (low LogR, top rows) enrichment of gene transcript (see Method section and reference 23), consistent with other large-scale categorization of cellular origin approaches (32). qPCR p and alr values correspond to MDD/UCMS samples.

^b Genes for which multiple probes were significantly and similarly affected in major depression and/or UCMS.